This article has been accepted for publication in IEEE Internet of Things Journal. This is the author's version which has not been fully edited and content may change prior to final publication. Citation information: DOI 10.1109/JIOT.2022.3232740

VariFi: Variational Inference for Indoor Pedestrian Localization and Tracking Using IMU and WiFi RSS

He Huang, Jianfei Yang, Xu Fang, Hao Jiang, and Lihua Xie, *Fellow, IEEE*

***Abstract*—Accurate indoor pedestrian localization and tracking are crucial in many practical applications. One efficient yet low-cost sensing scheme is the integration of IMU and WiFi RSS due to the popularity of smart devices and WiFi networks. Many approaches have been proposed to enhance the localization performance. However, they heavily rely on prerequisites including prior knowledge (e.g. map information) and beacon corrections, which degrades the generalization of the approaches and their accuracy in complex environments. To address this issue, in this paper, we propose a novel localization approach named VariFi, which incorporates variational inference techniques to estimate the location of pedestrian. Variational inference is applied in this work, whose inference network can produce accurate estimates as its parameters are optimized in terms of the reconstruction loss and regularization loss in real time. A signal map is constructed to provide a conditional RSS distribution at any given location, which is further applied to generate the reconstruction loss based on the real measurements. Also, a filtering mechanism is designed to reduce local optimum cases in optimization by utilizing the prior estimate and RSS fingerprinting estimate. In addition, VariFi can be further applied to conduct online optimization following the existing localization approaches. We conduct experiments including static localization and trajectory estimation scenarios to validate the performance of our approach. The trajectory estimation results show that our approach outperforms the mainstream approaches in terms of both localization accuracy and robustness, respectively. Furthermore, the combination of existing approaches and VariFi has also been validated effectively in the experiments of two environments, where VariFi has the ability to bring enhanced localization accuracy.**

***Index Terms*—Received Signal Strength (RSS), indoor localization, variational inference, signal map construction.**

I. Introduction

INDOOR pedestrian location services have gained much attention due to the increasing demand of relevant applications, e.g., indoor navigation, assistive living for visually impaired people, accurate odometry in virtual/augmented reality and contact tracing under the COVID-19 pandemic [1]. Since GPS has limited access in many indoor environments, alternative solutions have been studied by deploying other sensors [2], [3], [4], [5], [6]. However, some sensors still face challenges including high cost, portability, and low accuracy. Due to the popularity of smart devices and the development of wireless infrastructure, a smartphone equipped with inertial and WiFi sensors will be an ideal platform for a pedestrian localization system.

Pedestrian Dead Reckoning (PDR) method leverages data obtained by Inertial Measurement Unit (IMU) to detect walking steps, calculate the heading direction, and estimate the step length. Subsequently, the current position can be predicted based on the previous position and the movement information [7]. However, IMU sensors have drifting and biased errors, and are vulnerable to user's motions during walking. Apart from IMU, WiFi is another commonly used method for non-intrusive indoor localization [8], [9] and human perception [10], [11], [12]. Received Signal Strength (RSS) fingerprinting is the most popular method in WiFi based localization, which is usually comprised of an offline phase and an online phase. In the offline phase, RSS fingerprints (readings) are collected at known locations via site survey to build a database, which is used to train a designed model. While in the online phase, the real time captured RSS fingerprints will be fed to the trained model to estimate the user's position [8]. Nonetheless, RSS fingerprinting methods suffer from noise, co-channel interference, multipath propagation and other factors, which cause the variation of RSS and decreases the localization accuracy [13].

Many approaches integrating IMU and WiFi RSS have also been proposed to improve localization performance, among which Kalman Filter (KF) and Particle Filter (PF) are the popular choices. Analytical and optimization methods are commonly seen in Kalman filter based approaches, leading to less computation load. However, Kalman filter based methods cannot deal with high nonlinearity well, leading to instability during estimation. Particle filter based methods utilize weighted particles to fuse the results of the PDR and RSS fingerprinting to estimate the position by calculating the weighted sum of all particles. The weights of particles are usually determined by their consistency with the prior estimate, but seldom optimization schemes are used to estimate the results. Also, the weight degradation problem may weaken the localization performance [14]. Despite many existing methods fusing IMU and WiFi RSS, accurate and robust localization still remains an unsolved challenge.

To address this issue, in this paper, we propose VariFi, a novel indoor localization algorithm integrating IMU data from a smartphone and RSS fingerprints from WiFi Access Points (APs) to estimate the position of pedestrian. Different

H. Huang, J. Yang, X. Fang, and L. Xie are with the School of Electrical and Electronic Engineering, Nanyang Technological University, Singapore (E-mail: he008@e.ntu.edu.sg; yang0478@ntu.edu.sg; fa0001xu@e.ntu.edu.sg; elhxie@ntu.edu.sg).

H. Jiang is with the College of Electrical Engineering and Automation, Fuzhou University, Fuzhou, China (e-mail: jiangh@fzu.edu.cn).

*J. Yang is the corresponding author (e-mail: yang0478@e.ntu.edu.sg).

from previous filtering based methods, we incorporate the variational inference method into our algorithm to optimize the estimation process, which is inspired by the successful applications of Variational Auto-Encoder (VAE) in other Deep Learning fields [15]. Our motivation behind applying variational inference is that the localization problem should be better modelled in a probabilistic manner, because the RSS fingerprints obey some distribution at a given location and furthermore, an RSS fingerprint is always mapped to a potential region in the whole position space under a conditional distribution [16].

During position estimation, we still adopt PDR to obtain a prior estimate given the estimate of the last step, and then apply variational inference to optimize the position based on the prior estimate and real time RSS fingerprints. An inference network is designed to compute the posterior estimate given the RSS fingerprints, whose parameters are updated by the gradient descent learning algorithm in real time. Besides, we construct a signal radio map based on a modified Gaussian Process Regressor (GPR) method that provides predicted RSS fingerprints at the given position. The loss of optimization is evaluated as the log likelihood of the measured RSS under the reconstructed distribution generated by the signal map, together with the Kullback-Leibler (KL) divergence between the prior and posterior estimates. By minimizing the total loss, the optimization process can reach to convergence, with the parameters of the inference network being optimized by Adam [17] in this work. Following the optimization, a filter mechanism is introduced to reduce the local minimum cases. Furthermore, from a broader perspective, the proposed VariFi can also be deployed for localization applications purely using WiFi RSS data, i.e., to conduct online optimization toward existing localization approaches, and thus improve the localization accuracy.

The contributions of our work can be summarized as follows:

- We propose a novel approach for indoor localization based on IMU and RSS by modelling the location estimation as an optimization problem from the probabilistic perspective and dynamically optimizing the solution in real time.
- To the best of our knowledge, this work is also the first attempt to apply the variational Bayesian inference and gradient descent algorithm into the IMU and RSS based localization field.
- We implement several real experiments, which illustrate that our method outperforms the mainstream methods in terms of localization accuracy by up to 39.82%.
- We further expand the application of VariFi to optimize the results of existing approaches, which forms an offline-online dual optimization framework for WiFi RSS based localization. Experimental results show that the utilization of VariFi can help improve the localization accuracy.

The remainder of this paper is organized as follows. Section II introduces the related work. Section III provides the details of the proposed approach. Section IV shows the experimental results and comparison with different approaches. Section V explains the combination of the proposed method and existing localization approaches and the related improvements. Section VI concludes this paper.

II. Related Work

The proposed VariFi basically applies a prior-posterior estimate framework, which has been used in many previous works. As instances of such framework, Kalman filter, particle filter and their advanced variants are commonly seen in many researches. Different types of variational inference have also been applied into indoor localization field. In this section, we review recent techniques in these fields and introduce some background information of variational inference.

A. Kalman Filter and Particle Filter Based Schemes

Most approaches based on KF and PF apply PDR as the state update equation, whereas the state is updated later according to Kalman gain or filtering [1], [18], [14], [19], [20].

In Kalman filter based approaches, the position calculated by the PDR method serves as a prior estimate, at which the predicted RSS fingerprint is generated according to an observation model. Then the predicted RSS fingerprint is compared with the real time RSS measurements to compute the posterior estimate by making compensation (Kalman gain) to the prior estimate [21]. The observation function is usually set to be the Log Distance Path Loss (LDPL) model, so KF based approaches will obtain accurate results for linear or slightly nonlinear cases. However, there are many unpredictable factors (e.g. signal congestion, shadowing, interference, etc) in most real scenarios, resulting in the distortion of the observation function and the degraded performance. Kalman filter based methods perform well in linear or slightly nonlinear scenarios, but their performance will be largely degrade in highly nonlinear scenarios. There have been many research works proposed to enhance the performance. For example, landmarks (RSS readings at specific locations) are leveraged to restart the KF algorithm to avoid divergence [1]. Weighting mechanism and sampling method can be used to improve localization accuracy, but such method needs additional information (e.g. deployment of some iBeacons) to determine the weight of each candidate [22]. Nevetheless, the poor stability and low accuracy still hinder the application of KF based methods.

Different from using analytical methods for position estimation, particle filter applies a population based method to estimate the position, where the fitness value of each particle is computed and thus the weight is updated [14]. The final estimate of particle filter is calculated as the weighted sum of all particles. As a result, the performance of particle filter highly relies on the weight determination method. In [23], additional features (recognized turns, rooms and entrances) are used to constrain the weights, and thus improve the accuracy. Similarly, map information can also be utilized to constrain invalid particles by adjusting weights [24]. A new way for weight computation is to apply the reinforcement learning method, the sequence of an action can be evaluated and the weight of a particle can be updated [25]. Despite

This article has been accepted for publication in IEEE Internet of Things Journal. This is the author's version which has not been fully edited and content may change prior to final publication. Citation information: DOI 10.1109/JIOT.2022.3232740

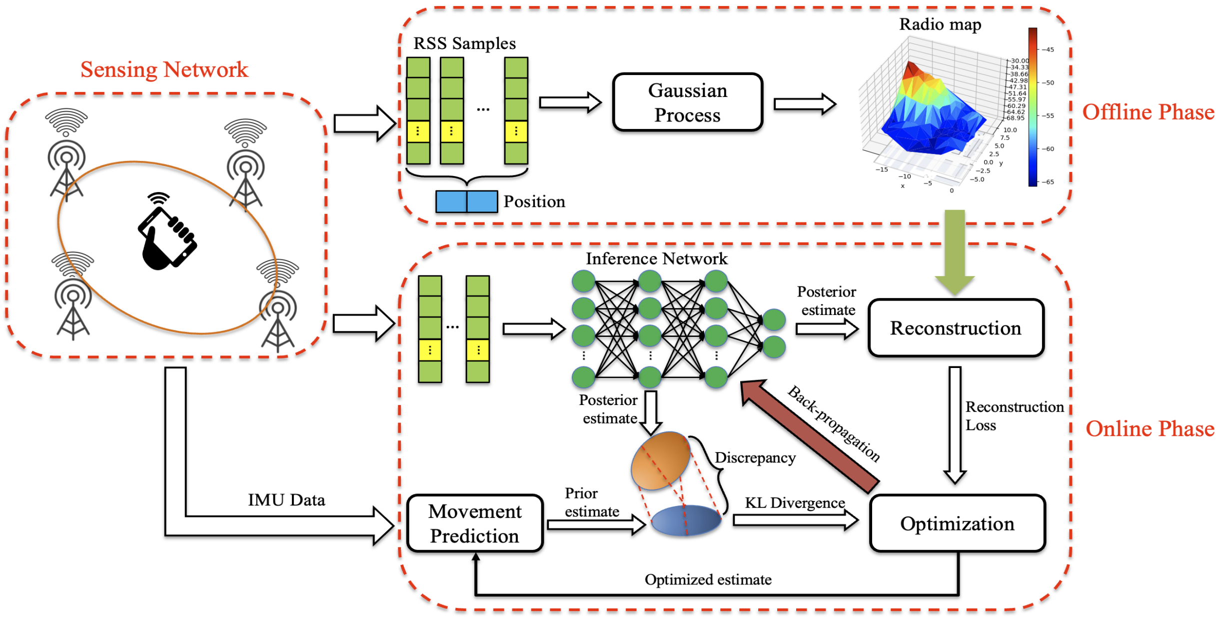

Fig. 1. The architecture of VariFi algorithm. The sensing network captures WiFi RSS data from several sensors, and the IMU data is collected on the smartphone. The offline phase is firstly conducted, where the collected position and RSS data are used to train a signal radio map. While in the online phase, the captured RSS data is fed into an inference network, whose result will be evaluated by the signal reconstruction and KL divergence between the prior estimate. The parameters of inference network will be optimized in real-time. When a new step is detected, the prior estimate is produced based on the optimized estimate and IMU data.

many previous works, how to determine weights still lacks theoretical support and is usually not optimized.

B. Variational Inference in Indoor Localization

Various methods applying variational inference have been proposed for different localization tasks in previous works [26], [27], [28]. Generally, for a system or process, the fundamental idea of variational inference is to approximate an intractable posterior distribution over a set of unobserved variables (also called state or latent variable) given some observed data by using the proposed variational distribution [29]. KL divergence is usually the default metric to evaluate the discrepancy between the two distributions, and the goal of variational inference is to minimize the KL divergence or optimizing the variational bound [30].

For problems solving a mapping relationship from input to output (e.g., classification, localization, etc), variational inference can provide another solution, in addition to the direct modelling and training method. For example, in [28], the authors introduce a set of latent feature vectors that behave as the driving factors for the whole localization process, wherein the sensory data and position at a location are regarded as some mapping outputs from the latent feature vector associated with the specific location. Moreover, in state-space models, the unobserved variable can be seen as the state to estimate. In [26], the sensor node location is estimated by the application of a mean-field variational inference algorithm, where the KL divergence is modeled and minimized iteratively.

Despite many related localization works, the applications of variational inference are either too complicated in offline training phase or not accurate enough in online localization. Hence, more accurate performance of variational inference is desired for online localization.

III. System Design

This section presents the technical details of each component in our proposed approach VariFi, whose architecture is given in Fig. 1. As usual, the whole procedure generally consists of two phases: an offline training phase and an online localization phase. In the offline training phase, an RSS database is built by collecting RSS fingerprints at reference points, followed by the construction of signal radio maps. The signal map is constructed by a modified GPR method, which can provide a conditional RSS distribution at the given position. In the online localization phase, three processes are designed for localization. The step prediction process receives the IMU data sent from a smartphone for new step detection, step length estimation and walking direction estimation, which are further used by the PDR method to provide a prior estimate based on the final estimate of the last step. The optimization process implements the variational inference method to optimize the posterior estimate, which is also the output of an inference network. The reconstruction loss is produced from the signal map and regularization loss is generated by the comparison of the prior estimate and posterior estimate. The filtering process handles the result of optimization by reducing local optimum cases where the prior estimate and RSS fingerprinting estimate are utilized to generate the final estimate.

A. Problem Formulation

IMU-RSS based localization problem can be modeled as a state estimation problem. In the localization problem, the unobservable state $z = (x, y)$ will be updated along pedestrian steps, which is also denoted by z_k at time step k. Also, let us consider the measured RSS dataset $R_k = \{r_k^{(i)}\}_{i=1}^{N_k}$ which consists of N_k RSS fingerprints during the time step k, and $r_k \in \boldsymbol{R}^M$ represents the RSS measurement from M WiFi APs. For the sake of simplicity, we just use r_k as the general RSS fingerprint in the following algorithm description. Thus, the problem can be modelled by

$$\begin{aligned} z_k &\sim f_k(z|z_{k-1}), \\ r_k &\sim h_k(r|z_k), \end{aligned}$$

where f_k is the state transition that can be measured by displacement sensors, such as IMU. h_k means the real RSS distribution which can be modelled through machine learning techniques given the dataset. In addition, for a given measured RSS r_k, the corresponding real position always has the following relationship.

$$z_k \sim p_{\theta_k}(z|r_k),$$

where θ_k represents the potential parameters for the real mapping relationship.

Our goal is to estimate the position z_k with high accuracy. For such a problem, we always assume the state transition f_k is accessible given the movement information. A modelled g_k is applied to simulate the real RSS measurement h_k. While for the intractable real relationship p_{θ_k}, we design an estimator called q_{ϕ_k} to compute the estimate $\hat{z}_k$. So the estimator can be formulated as

$$\begin{aligned} \tilde{z}_k &\sim f_k(z|\hat{z}_{k-1}^*), \\ \hat{r}_k &\sim g_k(r|\hat{z}_k), \\ \hat{z}_k &\sim q_{\phi_k}(z|\tilde{z}_k, r_k, \hat{r}_k), \end{aligned}$$

where $\tilde{z}_k$ denotes the prior estimate obtained by PDR and $\hat{z}_{k-1}^*$ means the optimal posterior estimate in step $k-1$. $\hat{r}_k$ is the predicted RSS fingerprint, which will be used to compare with the real RSS fingerprint r_k to calculate the posterior estimate $\hat{z}_k$ in the estimation model q_{θ_k}.

B. Pedestrian Dead Reckoning

The movement of a pedestrian can be detected by IMU sensors (accelerometer, gyroscope and magnetometer) on the smartphone, whose signals can be double-integrated into the displacement information. PDR uses the previous position and the displacement (step length and walking direction) to estimate the current position, thus the state transition $\tilde{z}_k \sim f_k(z|\hat{z}_{k-1}^*)$ can be further expanded as

$$\begin{aligned} \tilde{z}_k &\sim \mathcal{N}(\tilde{\mu}_k, \tilde{\sigma}_k^2), \\ \tilde{\mu}_k &= \hat{z}_{k-1}^* + l_k \begin{bmatrix} \sin(\theta_k) \\ \cos(\theta_k) \end{bmatrix}, \end{aligned} \tag{1}$$

where l_k and θ_k represent the step length and walking direction at time step k, and $\tilde{\sigma}_k^2$ is the covariance of prior estimate.

Some prior works on PDR have shown that there will be periodic changes on the vertical acceleration signal when feet hit the ground during walking, so we apply a threshold method to identify new steps. To estimate the walking length l_k, we adopt the method proposed in [31] which makes use of the vertical acceleration signal change and a calibration method. The walking direction can be provided by either the magnetometer or the gyroscope. However, magnetometer measurement suffers from magnetic field interference caused by the existence of other metals and electronic devices, and the gyroscope measurement has much noise that may be integrated into drifting errors. Therefore, we apply the commonly used EKF to fuse these two sensors for a better estimation of the walking direction.

C. Signal Map Construction

In this work, the signal map generates predicted RSS fingerprints at an arbitrary position, which is also called the reconstruction of measurement. Due to the presence of noise, interference and multipath effects, the ideal log-distance path loss model is no longer suitable to predict the RSS distribution precisely [32]. Instead, the nonparametric GPR method is applied to capture the statistical features of the RSS distribution and predict RSS fingerprints [9]. Nonetheless, original Gaussian process assumes zero mean function, which is obviously impractical for RSS prediction. Thus, a mean function should be pre-defined in advance to estimate the mean RSS value. Among the enormous choices, we adopt a polynomial surface function to predict the mean, which can be expressed by (For the sake of simplicity, we omit the subscript k in this subsection.)

$$\lambda(z) = \alpha_0 + \alpha_1 x + \alpha_2 y + \alpha_3 x^2 + \alpha_4 y^2 + \alpha_5 xy,$$

where $z = (x, y)$ is the coordinate of the position. It is worth noting that there are two reasons for choosing such function. First, the polynomial function can well fit the trend of RSS distribution (results can be referred in Section IV-E). Second, since the reconstruction evaluation follows the inference network whose parameters need to be optimized by gradient descent algorithm, the selected mean function should be friendly for gradient computation. The parameters $\{\alpha_i, 1 \leq i \leq 5\}$ can be approximated by fitting the collected data with the commonly used Least Squared Error (LSE) method. With the mean value of RSS, the residual RSS error can be computed by GPR.

Suppose we have collected a database $D^\tau = (Z^\tau, R^\tau)$ in which Z^τ and R^τ denote the location coordinates and the related RSS fingerprints at selected reference points. Then for an arbitrary position z_*, the GPR can be written by

$$\begin{bmatrix} R^\tau \\ r_* \end{bmatrix} \sim \mathcal{N}\left(\begin{bmatrix} \lambda(Z^\tau) \\ \lambda(z_*) \end{bmatrix}, \begin{bmatrix} K(Z^\tau, Z^\tau) + \sigma_g^2 I & K(Z^\tau, z_*) \\ K(z_*, Z^\tau) & K(z_*, z_*) \end{bmatrix} \right),$$

where σ_g^2 is the variance of RSS prediction noise and $K(\cdot, \cdot)$ denotes the covariance matrix of the predicted RSS fingerprints, whose elements are all of the squared exponential kernel form, given by

$$\kappa(z, z') = \sigma_f^2 \exp(-\frac{1}{2\gamma^2}(z - z')^2),$$

where σ_f^2 and γ control the vertical variation and horizontal length scale, respectively. Finally, the predicted RSS at z_* is calculated by

$$r_* \sim \mathcal{N}(m(z_*), v(z_*)), \tag{2}$$

where

$$\begin{aligned} m(z_*) &= \lambda(z_*) + \Sigma(z_*, Z^\tau)(R^\tau - \lambda(Z^\tau)), \\ v(z_*) &= K(z_*, z_*) - \Sigma(z_*, Z^\tau)K(Z^\tau, z_*), \\ \Sigma(z_*, Z^\tau) &= K(z_*, Z^\tau)[K(Z^\tau, Z^\tau) + \sigma_g^2 I]^{-1}. \end{aligned}$$

Note that the aforementioned prediction is for single dimensional RSS of one AP. Since the WiFi APs are deployed separately, the elements inside the RSS vector are i.i.d. (independent and identically distributed) with each others. As a result, for an RSS vector $r_k = (r_{k,1}, r_{k,2}, ..., r_{k,M})$, we have $p(r_k) = \prod_{i=1}^{M} p(r_{k,i})$, which indicates the prediction of the RSS vector can be decomposed into separate predictions of single RSS value. Thus, the RSS prediction can be written by

$$\hat{r}_k \sim g_k(r|\hat{z}_k) = \prod_{i=1}^{M} p(r_{k,i}|\hat{z}_k), \tag{3}$$

where

$$p(r_{k,i}|\hat{z}_k) = \mathcal{N}(m_i(\hat{z}_k), v_i(\hat{z}_k)), \quad \text{for } 1 \le i \le M.$$

Through the GPR, we can obtain a conditional distribution over the possible region of RSS. When the signal map is applied for position inference, it is not necessary to take the above computation everywhere, but just for those positions of interest. For z_k with known r_k, a smaller $\|r_k - \hat{r}_k\|$ implies that the estimate $\hat{z}_k$ is more similar to the ground truth z_k given the assumption that the signal map is constructed precisely. Hence, the similarity between $\hat{z}_k$ and z_k can be evaluated by $g_k(r_k|\hat{z}_k)$ or its logarithmic form $\log g_k(r_k|\hat{z}_k)$.

D. Inference and Optimization

Since the real position z_k is unknown, we adopt the estimated position $\hat{z}_k$ to approximate it, which in fact is equivalent to making estimator q_{ϕ_k} approach p_{θ_k}. The common way to evaluate the discrepancy between two distributions is the KL divergence. According to the definition of KL divergence, q_{ϕ_k} is equivalent to p_{θ_k} if and only if $D_{KL}(q_{\phi_k}(z|r_k)\|p_{\theta_k}(z|r_k)) = 0$, which is also the goal of inference. However, $D_{KL}(q_{\phi_k}(z|r_k)\|p_{\theta_k}(z|r_k))$ cannot be computed directly because the p_{θ_k} is intractable. What's more, the only variable we can access is the real RSS fingerprint r_k. Thus, we apply the way introduced in [15] to establish another relationship containing the KL divergence, which can be expressed by

$$\begin{aligned} \log p_{\theta_k}(r_k) &= E_{q_{\phi_k}(z|r_k)}\left[\log \frac{p_{\theta_k}(z, r_k)}{p_{\theta_k}(z|r_k)}\right] \\ &= D_{KL}(q_{\phi_k}(z|r_k)\|p_{\theta_k}(z|r_k)) + L(\theta_k, \phi_k; r_k), \end{aligned} \tag{4}$$

where $L(\theta_k, \phi_k; r_k)$ is called the variational lower bound of the marginal likelihood of the RSS measurement, which can be further expanded as

$$\begin{aligned} L(\theta_k, \phi_k; r_k) &= \int q_{\phi_k}(z|r_k) \log \frac{p_{\theta_k}(z, r_k)}{q_{\phi_k}(z|r_k)}\, dz \\ &= -D_{KL}(q_{\phi_k}(z|r_k)\|p_{\theta_k}(z)) \\ &\quad + E_{q_{\phi_k}(z|r_k)}\left[\log p_{\theta_k}(r_k|z)\right]. \end{aligned} \tag{5}$$

In (4), we can first apply the Bayesian law on the real mapping relationship p_{θ_k}, then take expectation of the expanded logarithmic marginal likelihood under the distribution of the proposed estimator $q_{\phi_k}(z|r_k)$. After simplification, we get the required KL divergence and another lower bound. From (4), it is obvious that when the KL divergence $D_{KL}(q_{\phi_k}(z|r_k)\|p_{\theta_k}(z|r_k))$ equals zero, the lower bound $L(\theta_k, \phi_k; r_k)$ achieves its maximum. In this sense, the optimization goal becomes maximizing $L(\theta_k, \phi_k; r_k)$.

The first Right-Hand-Side (RHS) term in (5) is a negative KL divergence of the posterior estimate from the prior, which behaves as a regularizer, while the second RHS term is the evaluation of posterior estimate, which is also called reconstruction. By maximizing the $L(\theta_k, \phi_k; r_k)$, our estimator $q_{\phi_k}(z|r_k)$ will gradually approximate the $p_{\theta_k}(z|r_k)$ and we can obtain an accurate estimate of real position z_k.

In our approach, the estimator $q_{\phi_k}(z|r_k)$ is assumed to follow a Gaussian-like conditional distribution, so it can be decomposed into two parametric functions: a mean function and a variance function described by

$$\hat{z}_k \sim q_{\phi_k}(z|r_k) = \mathcal{N}(\mu_{\phi_k}(r_k), \sigma^2_{\phi_k}(r_k)),$$

where $\mu_{\phi_k}(r_k)$ and $\sigma_{\phi_k}(r_k)$ represent the expectation and standard deviation of the posterior estimate, respectively. Since the real mapping relationship between position and RSS fingerprint is always highly nonlinear, neural network will be an ideal choice for posterior inference. For better real-time performance, we use a MultiLayer Perceptron (MLP) network as the structure for both the $\mu_{\phi_k}(r_k)$ and $\sigma_{\phi_k}(r_k)$. It is worth noting that, in the offline phase, the parameters of MLPs will not be trained, which are actually optimized in online inference phase.

Since the reconstruction term $E_{q_{\phi_k}(z|r_k)}\left[\log p_{\theta_k}(r_k|z)\right]$ cannot be computed analytically, the Monte Carlo Sampling method is applied to approximate the posterior $q_{\phi_k}(z|r_k)$, and S samples are randomly generated $\hat{z}_k^{(i)} \sim \mathcal{N}(\mu_{\phi_k}(r_k), \sigma_{\phi_k}(r_k))$, $1 \le i \le S$. For the reconstruction likelihood $p_{\theta_k}(r_k|z)$, we can use its alternative $g_k(r_k|z)$ which is detailed above, because it can be well fitted with the collected database (Z^τ, R^τ). Thus, the computation of $E_{q_{\phi_k}(z|r_k)}\left[\log p_{\theta_k}(r_k|z)\right]$ with S generated samples can be written by

$$E_{q_{\phi_k}(z|r_k)}\left[\log p_{\theta_k}(r_k|z)\right] \simeq \frac{1}{S}\sum_{i=1}^{S} \log g_k(r_k|\hat{z}_k^{(i)}).$$

While for the KL divergence $D_{KL}(q_{\phi_k}(z|r_k)\|p_{\theta_k}(z))$, the prior of real state $p_{\theta_k}(z)$ is usually assumed to be zero mean random signals in generative models. However, in this approach where the state refers to the position, zero mean prior estimate is impractical. Instead, we incorporate the position predicted in (1) to serve as the prior estimate for kth walking step estimation. Moreover, under the assumption of Gaussian-like posterior, we can compute the KL divergence $D_{KL}(q_{\phi_k}(z|r_k)\|p_{\theta_k}(z))$ in the analytical manner. Consequently, after Monte Carlo Sampling, the computation of the lower bound can be simplified to

$$L(\theta_k, \phi_k; r_k) \simeq \frac{1}{2}\sum_{j=1}^{J}\left(1 - \log\frac{\tilde{\sigma}_j^2}{\sigma_{\phi_k,j}^2} - \frac{\sigma_{\phi_k,j}^2}{\tilde{\sigma}_j^2} - \frac{(\mu_{\phi_k,j} - \tilde{\mu}_j)^2}{\tilde{\sigma}_j^2}\right) + \frac{1}{S}\sum_{i=1}^{S}\log g_k(r_k|\hat{z}_k^{(i)}), \tag{6}$$

where J is the dimension of the state z and $\hat{z}_k^{(i)}$ is the sample from $\mathcal{N}(\mu_{\phi_k}(r_k), \sigma_{\phi_k}(r_k))$. Therefore, the optimization can be further summarized as the following maximization problem during the walking step k.

$$\max_{\phi_k} L(\theta_k, \phi_k; r_k). \tag{7}$$

Given the captured RSS dataset $R_k = \{r_k^{(i)}\}_{i=1}^{N_k}$ during step k and the prior estimate $\tilde{z}_k$, we usually convert the maximization problem into a minimization problem and apply stochastic optimization methods such as Adam [17] to solve the optimization problem. As a result, the optimal parameter set ϕ_k^* is obtained, and the posterior estimate will be the mean value $\mu_{\phi_k^*}(r_k)$ with the optimal parameters, which can be expressed as

$$\hat{z}_k^* = \mu_{\phi_k^*}(r_k). \tag{8}$$

E. Filtering Mechanism

Previous sections have stated the main procedure of our approach, and the variational inference can achieve accurate results for localization. However, the result has the risk of falling into local optimums, where the gradients become nearly zero, but the estimated position is not near the real position.

To cope with this potential issue, we propose a filtering mechanism to reduce the local optimum cases following the optimization process. Since the optimized estimate may be a local optimum, we can also incorporate the prior estimate $\tilde{z}_k$ and RSS fingerprinting estimate z_k^R to improve the performance, which is produced by the Weighted K Nearest Neighbors (WKNN) method in this work. A filtering mechanism is designed to help reduce local optimum cases, in which a filtering region is selected after the optimization and some samples are generated to find the optimal estimate. The region is defined as a rectangle U_k whose boundaries are determined by z_k^R, $\tilde{z}_k$ and $\hat{z}_k^*$. The lower left point $z_k^l = (x_k^l, y_k^l)$ and top right point $z_k^t = (x_k^t, y_k^t)$ are calculated by

$$\begin{aligned} x_k^l &= \min(x_k^F - \tau, \hat{x}_k^* - \tau), \\ y_k^l &= \min(y_k^F - \tau, \hat{y}_k^* - \tau), \\ x_k^t &= \max(x_k^F + \tau, \hat{x}_k^* + \tau), \\ y_k^t &= \max(y_k^F + \tau, \hat{y}_k^* + \tau), \end{aligned}$$

where

$$\begin{aligned} x_k^F &= \frac{\tilde{x}_k + x_k^R}{2}, \\ y_k^F &= \frac{\tilde{y}_k + y_k^R}{2}. \end{aligned}$$

τ is the tolerance value. Subsequently, this filtering region is divided into C disjoint sub areas with the same size, i.e., $U_k = \cup_{i=1}^{C} u_k^{(i)}$. We denote the center of $u_k^{(i)}$ as $v_k^{(i)}$, and the weight of $u_k^{(i)}$ can be calculated by

$$w_k^{(i)} = \frac{\frac{1}{l(v_k^{(i)})}}{\sum_{i=1}^{C}\frac{1}{l(v_k^{(i)})}},$$

where $l(v_k^{(i)}) = ||v_k^{(i)} - \tilde{z}_k|| - \log g_k(x_k|v_k^{(i)})$ is the loss of the center $v_k^{(i)}$, and thus the weight $w_k^{(i)}$ can reflect the likelihood of the occurrence of the global posterior in sub area $u_k^{(i)}$. Finally, the optimal posterior estimate is updated through the filter, which can be expressed by

$$\hat{z}_k^* = \sum_{i=1}^{C} w_k^{(i)} v_k^{(i)}. \tag{9}$$

The whole procedure can be summarized in Algorithm 1.

IV. Experiments and Evaluation

A. Experimental Setup

1) Environment: To evaluate the performance of our proposed approach, we conduct experiments in a real world laboratory environment with different functional areas, as shown in Fig. 2. In this $20m \times 17m$ site, many desks and cabinets

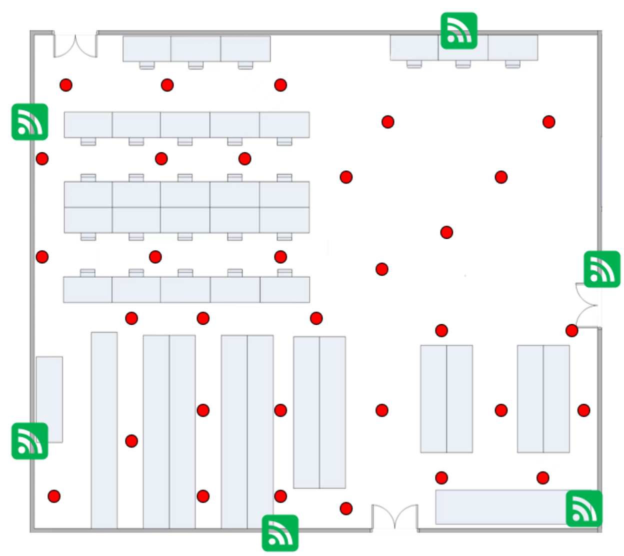

Fig. 2. The map and layout of the laboratory.

are deployed, which heavily obstruct the signal transmission, resulting in a Non-Line-of-Sight (NLOS) case. The green tags represent the 6 deployed WiFi APs that behave as sniffers and the red dots are the reference points where we record ground truth positions and their associated RSS fingerprints to construct the database $D^\tau = (Z^\tau, R^\tau)$. The database consists of 32 locations with 8 smoothed RSS fingerprints collected per location.

This article has been accepted for publication in IEEE Internet of Things Journal. This is the author's version which has not been fully edited and content may change prior to final publication. Citation information: DOI 10.1109/JIOT.2022.3232740

Algorithm 1: The Procedure for the Proposed Approach

Input:
D^τ - The collected database
K - The number of neighbors in WKNN
τ - The filtering tolerance
C - The number of disjoint subareas
Γ - The maximal iterations for optimization at each step
Output:
$\hat{z}_k^*$ - The estimated position
Initialization: $k = 0$
Construct the signal radio map $g(r|z)$
Compute the estimate of WKNN z_0^R
if *Initial estimate* z_{init} *is given* **then**
  $\tilde{z}_0 \leftarrow z_{init}$
else
  $\tilde{z}_0 \leftarrow z_0^R$
end
Running: $k \geq 1$
if *new step* **then**
  $l_k, \theta_k \leftarrow$ EKF(Acceleration)
  $\tilde{z}_k \leftarrow f_k(z|\hat{z}_{k-1}^*)$
  while $i \leq \Gamma$ *and Not Converged* **do**
    $L_1(\theta_k, \phi_k; r_k) \leftarrow \frac{1}{S}\sum_{i=1}^{S} \log g_k(r_k|\hat{z}_k^{(i)})$
    $L_2(\theta_k, \phi_k; r_k) \leftarrow$ KLDiv$(\tilde{z}_k, \hat{z}_k)$
    $L(\theta_k, \phi_k; r_k) \leftarrow L_1(\theta_k, \phi_k; r_k) + L_2(\theta_k, \phi_k; r_k)$
    Optimize ϕ_k by maximizing $L(\theta_k, \phi_k; r_k)$
  end
  $\hat{z}_k^* \leftarrow \mu_{\phi_k^*}(r_k)$
  $z_k^R \leftarrow$ WKNN(r_k)
  $\hat{z}_k^* \leftarrow$ Filter$(z_k^R, \tilde{z}_k, \hat{z}_k^*; \tau)$
end

2) Baselines: We select the following four methods as baselines: 1) *IMU based method*: PDR; 2) *RSS fingerprinting method*: WKNN; 3) *KF based method*: UKF; 4) *PF based method*: PF [33].

3) Parameters: For the prior estimate, we set the covariance of prior $\tilde{\sigma}_k^2$ as a 2-D constant identity matrix. For the posterior estimator, a 5-layer neural network (three fully connected layers and two activation layers) is selected to be the structure for both the mean and covariance functions, whose hidden layer sizes are 16, 8, and 2, respectively. The adopted activation functions are the Parametric Rectified Linear Unit (PReLU). We initialize the parameters of inference neural networks ϕ_0 randomly before the beginning of walking, and set the initial learning rate as 10^{-2} and optimizer as Adam. The maximal number of iterations Γ for each step's optimization is 100. For the filtering mechanism, 25 disjoint areas are applied and the tolerance τ is set to be $1m$. The walking speed of the pedestrian ranges from $1.0m/s$ to $1.2m/s$, and all the computation is taken on a laptop platform with only an AMD R5 3550H CPU in real time.

TABLE I
OVERALL LOCALIZATION ERRORS OF DIFFERENT METHODS IN THE TRAJECTORY ESTIMATION.

Methods	MAE (m)	Standard Deviation (m)	Worst-case Error (m)
PDR	3.185	0.883	5.255
WKNN	2.725	0.596	3.533
UKF	2.387	0.408	4.875
PF	1.921	0.979	4.374
VariFi	1.156	0.318	2.549

B. Comparison with Baselines

For comparison of the localization accuracy in complex scenarios, a pedestrian walks along a closed trajectory surrounded with cubicles and desks. Since there is uncertainty in each trial, 24 trials are taken for each method along the same trajectory so that the robustness of different methods can be studied. The walking process takes an average of 102 steps, but 94 steps are detected by the IMU data indicating that there will be missing estimations in the methods that apply PDR. We use the Mean Absolute Error (MAE) to evaluate the localization accuracy. The overall mean error and the standard deviation of each method are reported in Table I.

From Table I, we can observe that our proposed method outperforms other compared methods in terms of both localization accuracy and robustness, achieving the least mean localization error and standard deviation. The mean localization error of the proposed method is $1.156m$, which gains improvements of 39.82% and 51.57% compared to PF and UKF, respectively. Also, the proposed method gets the least worst-case error in all the compared methods, which means our method can maintain strong robustness while achieving high accuracy. Moreover, Fig. 3 shows the details of the estimated trajectories of our proposed method and the baselines on the same closed trajectory. The errors with respect to steps for all the compared methods are displayed in Fig. 4. In Fig. 3(a), it is obvious that the PDR method suffers from large biased and drifting errors as the average PDR estimated trajectory deviates from the real path. Also, the RSS fingerprinting estimates cannot reflect the movement of the pedestrian since some estimates locate close to each other while the pedestrian keeps walking.

From Fig. 3(b) to Fig. 3(d), we can see that the estimated trajectory of the proposed method best matches the real path compared to UKF and PF methods. It is noticeable that all the estimates for the first part (trajectory from the starting point to the first corner) deviate from the real path to some extent, which is caused by the drifting of IMU and high similarity of RSS fingerprints for the points in the region. But from the first corner, all the estimated trajectories gradually approximate the real path, in which our proposed method gets the smoothest and most stable results. This can be also observed from Fig. 4 where the proposed method obtains the least errors for most steps.

In addition, the proposed method can still estimate the positions with high accuracy in areas nearing the boundaries of the environment (e.g., from the upper left corner near the door to the ending point), whereas the other compared methods get

This article has been accepted for publication in IEEE Internet of Things Journal. This is the author's version which has not been fully edited and content may change prior to final publication. Citation information: DOI 10.1109/JIOT.2022.3232740

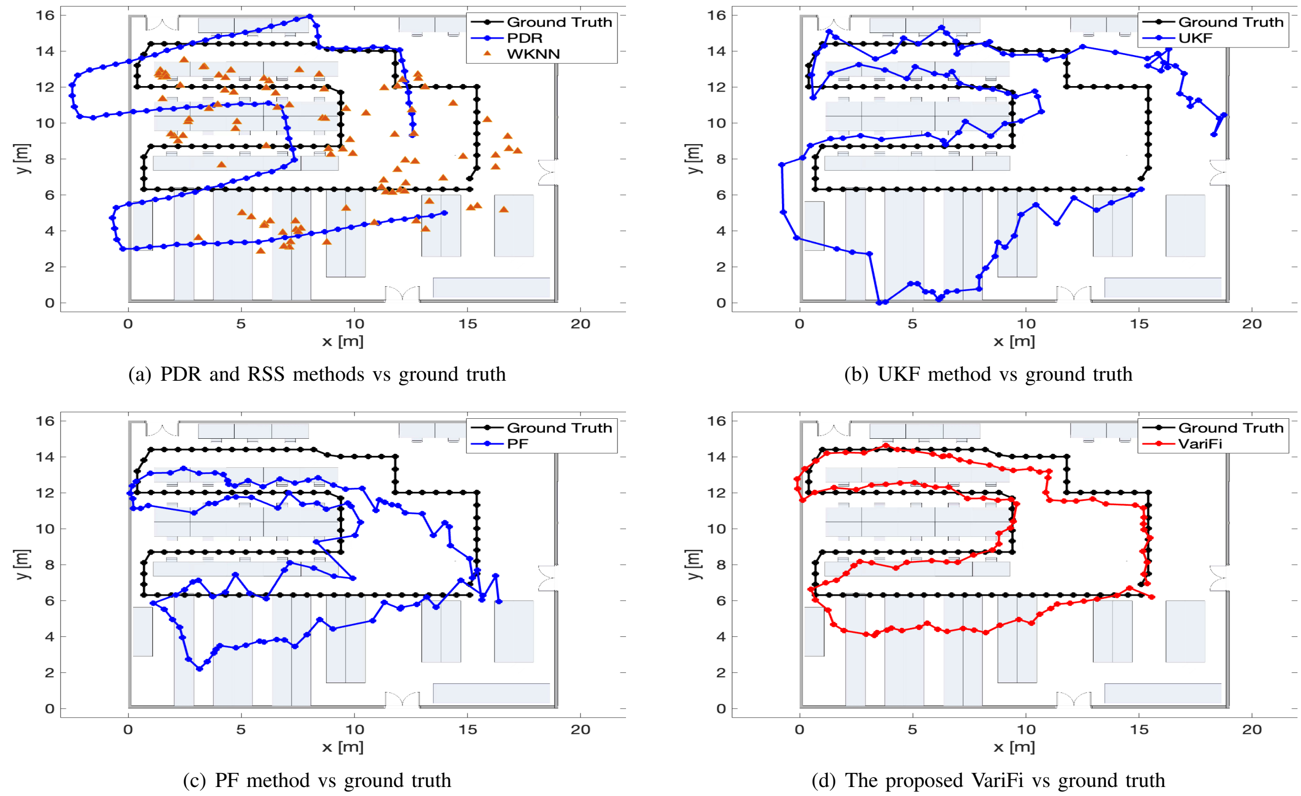

(a) PDR and RSS methods vs ground truth

(b) UKF method vs ground truth

(c) PF method vs ground truth

(d) The proposed VariFi vs ground truth

Fig. 3. Comparisons of estimated trajectories from different approaches.

distorted estimation. This indicates that the proposed method has the capability of handling the localization difficulties caused by the complexity of environment, biased error in IMU and uncertainty in RSS. We believe that, the improvement of accuracy in WiFi localization can be attributed to the precise construction of signal maps and nonlinear optimization that is better solved by variational inference through the utilization of neural networks, whereas conventional approaches are not able to tackle these issues well.

For more details of the robustness comparison, the Cumulative Density Function (CDF) of localization error for the five methods are displayed in Fig. 5.

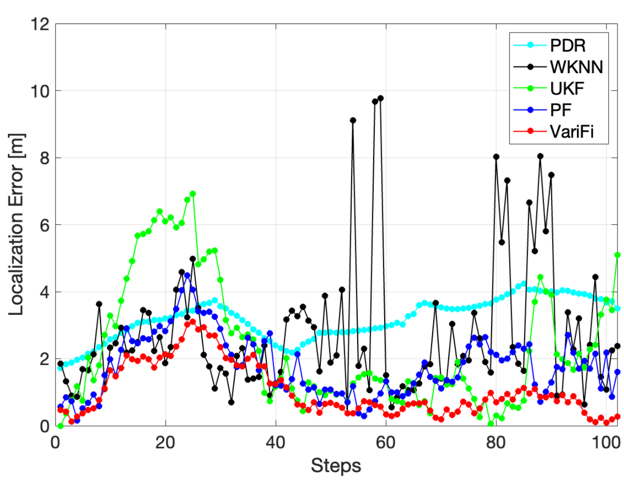

Fig. 4. Localization errors with respect to each step.

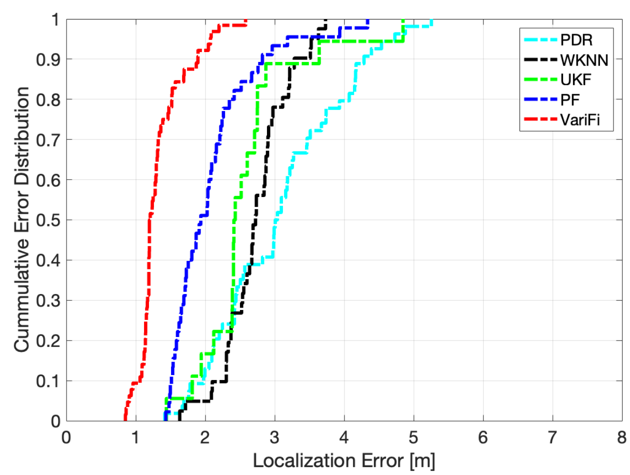

Fig. 5. Cumulative error distribution of different methods.

C. Optimization Performance

To study the performance of optimization, we conduct some experiments at several fixed points and record the information including the current estimate and loss during the optimization process. The testing points (ground truth) are selected to be $(12.4, 2.4)$, $(15.4, 8.4)$ and $(2.2, 12.0)$, respectively. At each testing point, we assume the prior estimate $\tilde{z}$ to be away from the real position z with a distance of $1.0m$. The parameters of the inference network are kept the same as those in the trajectory estimation and the learning rate is set as 10^{-2} initially that gradually decays to 10^{-3}. Fig. 6 illustrates the optimization

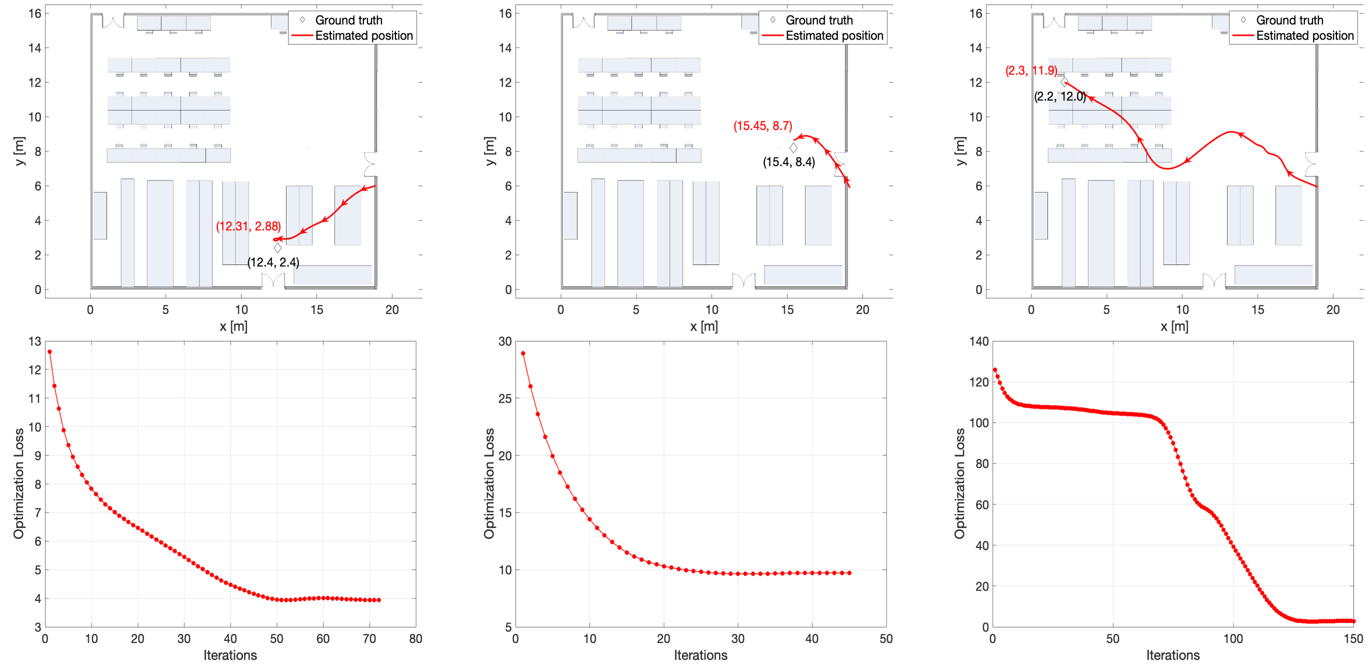

(a) Convergence trajectory and optimization loss at (12.4,2.4)

(b) Convergence trajectory and optimization loss at (15.4,8.4)

(c) Convergence trajectory and optimization loss at (2.2,12.0)

Fig. 6. Optimization process at several fixed points. The red arrowed lines in the upper figures represent the posterior estimates during the optimization process. Note that the initial posterior estimates of all the above processes start from the right door. This is because the parameters of inference networks are very small at the beginning, and the right door is the origin of coordinates in the code implementation.

process at these points. The converged optimization results are always within $0.5m$ of the real locations and the optimization loss will achieve minimum after several iterations, which indicates the effectiveness of the optimization process.

D. Computational Load Analysis

Although the proposed approach provides accurate localization results, the computational load should also be taken into consideration in implementation. Since we apply the variational inference method for localization that contains gradient descent based learning for parameter optimization, the process requires iterative computation whereas the conventional approaches take one-step computation for one estimate. However, more computation does not mean the approach is impractical, as the devices are usually equipped with computation resources nowadays, even for the edge devices. Hence, the computational load should be investigated for better reference in the future implementation. In this work, the iterations and time used for convergence at each step in the above trajectory are recorded and displayed in Fig. 7.

From Fig. 7, we can observe that for each step's estimation, the time used for convergence does not exceed $0.15s$ and the maximal number of iterations is 49. Considering that the time interval during two steps is much larger than $0.15s$ for most people, we can claim that the proposed algorithm can provide accurate localization services in real time. Moreover, it is worth noting that the computation is conducted on an AMD R5 3550H CPU (4 cores with frequency ranging from 2.1GHz to 3.0GHz) laptop without any GPU resources, which means the time used for convergence can be largely shorter on devices equipped with GPUs as the computational speed will be accelerated exponentially.

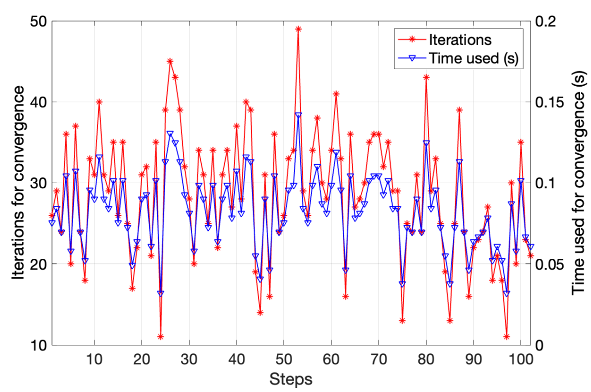

Fig. 7. The iterations and time required for convergence at each step.

E. Signal Map Comparison

The signal map constructed based on the modified GPR method provides metrics to evaluate whether the predicted RSS matches the real RSS in order to adjust the parameters of the estimator. From this point of view, a precise signal map is important to the proposed approach. In this work, we construct signal maps for each WiFi AP, some of which can be shown in Fig. 8. We can observe that the constructed signal maps can basically reflect the mean value of the RSS measurement.

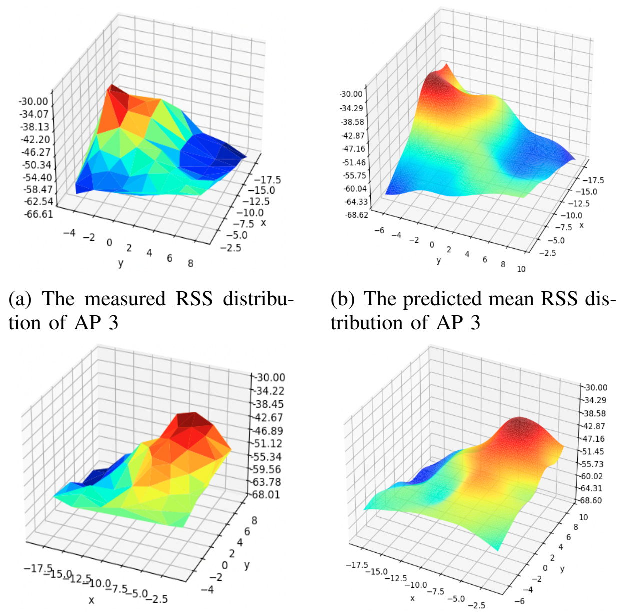

(a) The measured RSS distribution of AP 3

(b) The predicted mean RSS distribution of AP 3

(c) The measured RSS distribution of AP 6

(d) The predicted mean RSS distribution of AP 6

Fig. 8. Comparisons of the WiFi RSS radio maps.

TABLE II
COMPARISONS BETWEEN THE PREDICTED RSS FINGERPRINTS AND REAL RSS FINGERPRINTS.

AP Index	AP 1	AP 2	AP 3	AP 4	AP 5	AP 6
MAE (dB)	0.525	0.431	0.528	0.414	0.516	0.499

Besides, we compare the MAE between the real RSS values and predicted RSS values at all the 32 reference points for each WiFi AP, whose results can be shown in Table II.

F. Ablation Study

To study the effect of the filtering mechanism, we compare the complete method q_ϕ and the method without filtering $q_{\phi,f-}$. The comparison results are shown in Table III, where we can find the q_ϕ outperforms $q_{\phi,f-}$ in terms of both the mean accuracy and the standard deviation. For mean accuracy, q_ϕ achieves improvements of 23.42% and 11.69% over $q_{\phi,f-}$ for static and dynamic localization, respectively. For the standard deviation, it is obvious that in the dynamic localization, the performance of q_ϕ is more stable compared to $q_{\phi,f-}$ with a 39.08% improvement, which is higher than that in the static localization. We think this is caused by the utilization of RSS fingerprinting estimates. For different trials on the same trajectory, the IMU information may vary at the same location due to its sensitivity to human motions (e.g. hand shakes), against which the RSS fingerprinting estimates are stable. The prior estimate $\tilde{z}_k$ will influence the performance of optimization, which is predicted based on the estimated direction θ_k and the final estimate $\hat{z}^*_{k-1}$ at the last step. Although the IMU error is directly introduced into $\tilde{z}_k$, a more accurate $\hat{z}^*_{k-1}$ after filtering will reduce the variation of $\tilde{z}_k$, which enhances the robustness of the whole approach along steps. Therefore, the filtering mechanism is able to improve the localization accuracy and robustness.

TABLE III
COMPARISON OF THE PROPOSED METHOD WITH AND WITHOUT FILTERING.

Models	Static Localization		Dynamic Localization	
	Mean (m)	STD (m)	Mean (m)	STD (m)
$q_{\phi,f-}$	0.649	0.330	1.309	0.522
q_ϕ	0.497	0.281	1.156	0.318

V. OPTIMIZATION TOWARD EXISTING LOCALIZATION APPROACHES

In the above section, we have discussed the evaluation results on indoor human tracking in a multi-function laboratory. In the human tracking model, we utilize IMU data to predict the prior estimate upon the detection of a new human step. Then the optimization is conducted to produce the estimated position. In fact, the application of VariFi can be further expanded.

A. Offline-Online Dual Optimization

From a broader view, our proposed VariFi can be used to optimize the results of most localization methods. To be specific, since most machine learning and deep learning based approaches apply the train-test framework, optimization in these methods is only conducted toward the training data samples. As a result, during the testing phase, the estimated position is not optimized to be accurate enough. Our proposed VariFi can handle this problem by taking optimization in real time during the testing phase. As to technical implementation, the only difference is the replacement of prior estimate in VariFi. In detail, the prior estimate is produced by (1) with the assistance of IMU information. However, if we are only given RSS data for localization, we can just practice an existing indoor localization approach π with associated parameter set ρ, namely $z = \pi_\rho(r)$. In theory, π can be any approach based on the train-test framework. To make the optimization computable, the Gaussian-like prior assumption is still necessary. After obtaining the prior estimate provided by π_ρ, we can apply the above mentioned variational inference to compute the posterior estimate.

In summary, the offline-online dual optimization consists of two steps. Firstly, the selected approach π_ρ should be optimized using training dataset $D^\tau = (Z^\tau, R^\tau)$, yielding

$$\min_\rho \; loss(\rho) = MSE(Z^\tau, \pi_\rho(R^\tau)), \tag{10}$$

whose optimized parameter set is denoted by ρ^*. Secondly, without loss of generality, suppose that we capture an RSS sample, namely r_t in the testing phase. Then the prior estimate distribution can be produced by

$$\begin{aligned} \tilde{z} &\sim \mathcal{N}(\tilde{\mu}, \tilde{\sigma}^2), \\ \tilde{\mu} &= \pi_{\rho^*}(r_t), \end{aligned} \tag{11}$$

TABLE IV
MEAN LOCALIZATION ERRORS AND PERCENTAGE OF IMPROVEMENTS FOR ALL THE APPROACHES UNDER TWO ENVIRONMENTS.

Scenarios	Criterion	WKNN		DANN		RF		CNNLoc [34]		LF-DLSTM [35]	
		WKNN	+VariFi	DANN	+VariFi	RF	+VariFi	CNNLoc	+VariFi	LF-DLSTM	+VariFi
Laboratory	Error (m)	2.441	1.947	2.889	2.015	2.884	2.166	2.412	1.982	2.857	2.023
($20 \times 17m, M = 6$)	Improvement (%)	-	20.24%	-	30.25%	-	24.87%	-	17.83%	-	29.22%
Office room	Error (m)	1.656	1.472	1.928	1.710	2.067	1.830	1.956	1.752	1.763	1.693
($10 \times 5m, M = 3$)	Improvement (%)	-	11.11%	-	11.31%	-	11.47%	-	10.43%	-	3.97%

where $\tilde{\sigma}^2$ represents the estimate covariance of the approach π_ρ, which can be either obtained by user-tuning or computation from a cluster of estimated positions with Monte Carlo Sampling applied to the test RSS data. Once the prior estimate is got, the posterior estimate can be calculated according to

$$\begin{aligned} \hat{r} &\sim g(r|\hat{z}), \\ \hat{z} &\sim q_\phi(z|\tilde{z}, r_t, \hat{r}), \end{aligned} \tag{12}$$

where g is the RSS radio map constructed by the training dataset D^τ using the method introduced in Section III-C. Similarly, the variational lower bound $L(\theta, \phi; r_t)$ should be optimized, yielding

$$\begin{aligned} \max_\phi \ L(\theta, \phi; r_t) \simeq \frac{1}{2} \sum_{j=1}^{2} \Bigg(1 - \log \frac{\tilde{\sigma}_j^2}{\sigma_{\phi,j}^2} - \frac{\sigma_{\phi,j}^2}{\tilde{\sigma}_j^2} \\ - \frac{(\mu_{\phi,j} - \tilde{\mu}_j)^2}{\tilde{\sigma}_j^2} \Bigg) + \frac{1}{S} \sum_{i=1}^{S} \log g(r_t|\hat{z}^{(i)}), \end{aligned} \tag{13}$$

where $\hat{z}^{(i)} \sim \mathcal{N}(\mu_\phi(r_t), \sigma_\phi(r_t))$, $1 \leq i \leq S$. For the sake of simplicity, we refer to the combination of offline optimization approach π_ρ and online optimization approach q_ϕ as $\Omega_{\rho,\phi}$.

B. Evaluation and Comparison

To validate the improvement of VariFi on existing WiFi RSS based approaches, we select several localization schemes using WiFi RSS data, which include: 1). WKNN; 2). Deep Artificial Neural Network (DANN); 3). Random Forest Regression (RF); 4). CNNLoc [34]; 5). LF-DLSTM [35]. The configurations of the selected methods and VariFi are listed in Table V. *FC(20-Tanh)* means a fully connected layer whose output dimension and activation function are 20 and *Tanh*, respectively. *Conv(40-10-ELU)* means the convolutional layer has 40 output channels with the filter size of 10, and the activation function is *ELU*. Similarly, *LSTM(20-Sigmoid)* denotes an LSTM network with 20 dimensional output and *Sigmoid* as the gate function. It is worth noting that the configurations (hyper-parameters) of selected approaches are well tuned but not guaranteed to be optimized since the subject of this validation is the improvement brought by the application of VariFi toward existing approaches.

To better study the improvement of VariFi based on existing localization schemes, we also collect data from another office room environment of size $10m \times 5m$, where 3 WiFi APs are installed. Finally, the results and improvements are listed in Table IV. From the results, we can observe that VariFi can enhance the localization accuracy of existing approaches since it can optimize the inference in the online phase.

TABLE V
CONFIGURATIONS OF THE SELECTED APPROACHES.

Approach	Configuration
WKNN	K=5
ANN	Input→FC(20-Tanh)→FC(10-PReLU)→FC(2)
RF	50 estimators (trees)
CNNLoc	Input(1,5×M)→FC(64-ELU)→FC(32-ELU)→ Conv(40-10-ELU)→Conv(20-10-ELU)→Conv(10-5-ELU) →flatten→FC(40-ELU)→FC(2)
LF-DLSTM	Input(50,M)→Feature(5,5×M)→LSTM(20-Sigmoid) →LSTM(30-Sigmoid)→FC(60-ELU)→FC(2)
VariFi	Input→FC(15-PReLU)→FC(30-PReLU)→FC(10-PReLU) →FC(2)

It is also worth mentioning that compared to the laboratory environment, the performance improvement in the office room environment is degraded to some extent. We think it can be attributed to the reduction of information brought by radio maps. To be detailed, the constructed radio map for each WiFi module is used for position inference, through which the reconstruction loss is generated. Thus, the accuracy of radio map construction and numbers of deployed WiFi modules are the vital factors for improving localization performance in this framework. Only 3 WiFi modules are utilized in the office environment which provides less evaluation metrics for the optimization. So, it is reasonable that the performance improvement becomes smaller. In the future, we will also investigate how the parameters of radio maps can be updated against environmental changes for better transfer ability from one environment to another.

VI. CONCLUSION

In this paper, we proposed VariFi, a novel approach to provide accurate localization services for indoor pedestrians based on IMU and RSS measurements from smartphones and WiFi APs. We construct signal radio maps for different APs to model the relationship from the position to RSS fingerprints by the utilization of a modified GPR method. The variational inference method is incorporated into our approach to help optimize the estimated position through optimizing the parameters of the designed inference network with gradient descent based learning. The reconstruction loss is the evaluated by the predicted RSS distribution and measured RSS fingerprints, and the regularization loss is calculated by the similarity between the prior and posterior estimates. We further expand the application of VariFi to enable the offline-online dual optimization for WiFi RSS based localization, where VariFi is used to optimize the estimated results from existing localization approaches. The conducted experiments demonstrate that VariFi outperforms other compared approaches in terms of both the localization accuracy and robustness in the trajectory estimation test, validating the effectiveness of VariFi. Additional experiments from two environments also validate the effectiveness of VariFi when combined with existing localization methods, in which VariFi is shown to bring accuracy improvements toward all the compared approaches.

References

[1] Z. Chen, H. Zou, H. Jiang, Q. Zhu, Y. C. Soh, and L. Xie, "Fusion of wifi, smartphone sensors and landmarks using the kalman filter for indoor localization," *Sensors*, vol. 15, no. 1, pp. 715–732, 2015.

[2] S. Xu and W. Chou, "An improved indoor localization method for mobile robot based on wifi fingerprint and amcl," in *2017 10th International Symposium on Computational Intelligence and Design (ISCID)*, vol. 1. IEEE, 2017, pp. 324–329.

[3] W. Liu, D. Caruso, E. Ilg, J. Dong, A. I. Mourikis, K. Daniilidis, V. Kumar, and J. Engel, "Tlio: Tight learned inertial odometry," *IEEE Robotics and Automation Letters*, vol. 5, no. 4, pp. 5653–5660, 2020.

[4] S. Sun, D. Melamed, and K. Kitani, "Idol: Inertial deep orientation-estimation and localization," in *Proceedings of the AAAI Conference on Artificial Intelligence*, vol. 35, no. 7, 2021, pp. 6128–6137.

[5] H. Zou, Y. Zhou, J. Yang, and C. J. Spanos, "Unsupervised wifi-enabled iot device-user association for personalized location-based service," *IEEE Internet of Things Journal*, vol. 6, no. 1, pp. 1238–1245, 2018.

[6] H. Zou, H. Jiang, J. Yang, L. Xie, and C. Spanos, "Non-intrusive occupancy sensing in commercial buildings," *Energy and Buildings*, vol. 154, pp. 633–643, 2017.

[7] Z. Chen, Q. Zhu, and Y. C. Soh, "Smartphone inertial sensor-based indoor localization and tracking with ibeacon corrections," *IEEE Transactions on Industrial Informatics*, vol. 12, no. 4, pp. 1540–1549, 2016.

[8] J. Biswas and M. Veloso, "Wifi localization and navigation for autonomous indoor mobile robots," in *2010 IEEE international conference on robotics and automation*. IEEE, 2010, pp. 4379–4384.

[9] H. Zou, M. Jin, H. Jiang, L. Xie, and C. J. Spanos, "Winips: Wifi-based non-intrusive indoor positioning system with online radio map construction and adaptation," *IEEE Transactions on Wireless Communications*, vol. 16, no. 12, pp. 8118–8130, 2017.

[10] J. Yang, X. Chen, D. Wang, H. Zou, C. X. Lu, S. Sun, and L. Xie, "Deep learning and its applications to wifi human sensing: A benchmark and a tutorial," *arXiv preprint arXiv:2207.07859*, 2022.

[11] J. Yang, H. Zou, H. Jiang, and L. Xie, "Device-free occupant activity sensing using wifi-enabled iot devices for smart homes," *IEEE Internet of Things Journal*, vol. 5, no. 5, pp. 3991–4002, 2018.

[12] J. Yang, H. Zou, Y. Zhou, and L. Xie, "Learning gestures from wifi: A siamese recurrent convolutional architecture," *IEEE Internet of Things Journal*, vol. 6, no. 6, pp. 10 763–10 772, 2019.

[13] S. Sen, J. Lee, K.-H. Kim, and P. Congdon, "Avoiding multipath to revive inbuilding wifi localization," in *Proceeding of the 11th annual international conference on Mobile systems, applications, and services*, 2013, pp. 249–262.

[14] Z. Li, C. Liu, J. Gao, and X. Li, "An improved wifi/pdr integrated system using an adaptive and robust filter for indoor localization," *ISPRS International Journal of Geo-Information*, vol. 5, no. 12, p. 224, 2016.

[15] D. P. Kingma and M. Welling, "Auto-encoding variational bayes," *arXiv preprint arXiv:1312.6114*, 2013.

[16] Y. Gu, C. Zhou, A. Wieser, and Z. Zhou, "Pedestrian positioning using wifi fingerprints and a foot-mounted inertial sensor," in *2017 European Navigation Conference (ENC)*. IEEE, 2017, pp. 91–99.

[17] D. P. Kingma and J. Ba, "Adam: A method for stochastic optimization," *arXiv preprint arXiv:1412.6980*, 2014.

[18] Z.-A. Deng, Y. Hu, J. Yu, and Z. Na, "Extended kalman filter for real time indoor localization by fusing wifi and smartphone inertial sensors," *Micromachines*, vol. 6, no. 4, pp. 523–543, 2015.

[19] W. Wang, D. Marelli, and M. Fu, "Dynamic indoor localization using maximum likelihood particle filtering," *Sensors*, vol. 21, no. 4, p. 1090, 2021.

[20] H. Zou, Z. Chen, H. Jiang, L. Xie, and C. Spanos, "Accurate indoor localization and tracking using mobile phone inertial sensors, wifi and ibeacon," in *2017 IEEE International Symposium on Inertial Sensors and Systems (INERTIAL)*. IEEE, 2017, pp. 1–4.

[21] G. Chen, X. Meng, Y. Wang, Y. Zhang, P. Tian, and H. Yang, "Integrated wifi/pdr/smartphone using an unscented kalman filter algorithm for 3d indoor localization," *Sensors*, vol. 15, no. 9, pp. 24 595–24 614, 2015.

[22] K. Sung, D. K. Lee, and H. Kim, "Indoor pedestrian localization using ibeacon and improved kalman filter," *Sensors*, vol. 18, no. 6, p. 1722, 2018.

[23] F. Hong, Y. Zhang, Z. Zhang, M. Wei, Y. Feng, and Z. Guo, "Wap: Indoor localization and tracking using wifi-assisted particle filter," in *39th Annual IEEE Conference on Local Computer Networks*. IEEE, 2014, pp. 210–217.

[24] X. Du, X. Liao, Z. Gao, and Y. Fan, "An enhanced particle filter algorithm with map information for indoor positioning system," in *2019 IEEE Global Communications Conference (GLOBECOM)*. IEEE, 2019, pp. 1–6.

[25] J. L. C. Villacrés, Z. Zhao, T. Braun, and Z. Li, "A particle filter-based reinforcement learning approach for reliable wireless indoor positioning," *IEEE journal on selected areas in communications*, vol. 37, no. 11, pp. 2457–2473, 2019.

[26] B. Zhou, Q. Chen, H. Wymeersch, P. Xiao, and L. Zhao, "Variational inference-based positioning with nondeterministic measurement accuracies and reference location errors," *IEEE Transactions on Mobile Computing*, vol. 16, no. 10, pp. 2955–2969, 2016.

[27] J. N. Wong, D. J. Yoon, A. P. Schoellig, and T. D. Barfoot, "Variational inference with parameter learning applied to vehicle trajectory estimation," *IEEE Robotics and Automation Letters*, vol. 5, no. 4, pp. 5291–5298, 2020.

[28] M. Kim, D. Han, and J.-K. K. Rhee, "Multiview variational deep learning with application to practical indoor localization," *IEEE Internet of Things Journal*, vol. 8, no. 15, pp. 12 375–12 383, 2021.

[29] K. Zhou, C. Chen, B. Wang, M. R. U. Saputra, N. Trigoni, and A. Markham, "Vmloc: Variational fusion for learning-based multimodal camera localization," in *Proceedings of the AAAI Conference on Artificial Intelligence*, vol. 35, no. 7, 2021, pp. 6165–6173.

[30] N. Chu, Y. Ning, L. Yu, Q. Huang, and D. Wu, "A fast and robust localization method for low-frequency acoustic source: Variational bayesian inference based on nonsynchronous array measurements," *IEEE Transactions on Instrumentation and Measurement*, vol. 70, pp. 1–18, 2020.

[31] Y. Jin, H.-S. Toh, W.-S. Soh, and W.-C. Wong, "A robust dead-reckoning pedestrian tracking system with low cost sensors," in *2011 IEEE International Conference on Pervasive Computing and Communications (PerCom)*. IEEE, 2011, pp. 222–230.

[32] X. Wang, X. Wang, S. Mao, J. Zhang, S. C. Periaswamy, and J. Patton, "Indoor radio map construction and localization with deep gaussian processes," *IEEE Internet of Things Journal*, vol. 7, no. 11, pp. 11 238–11 249, 2020.

[33] H. Huang, J. Yang, X. Fang, H. Jiang, and L. Xie, "An improved pso approach to indoor localization system based on imu, wifi rss and map information," in *2022 IEEE 17th International Conference on Control & Automation (ICCA)*. IEEE, 2022, pp. 692–697.

[34] X. Song, X. Fan, C. Xiang, Q. Ye, L. Liu, Z. Wang, X. He, N. Yang, and G. Fang, "A novel convolutional neural network based indoor localization framework with wifi fingerprinting," *IEEE Access*, vol. 7, pp. 110 698–110 709, 2019.

[35] Z. Chen, H. Zou, J. Yang, H. Jiang, and L. Xie, "Wifi fingerprinting indoor localization using local feature-based deep lstm," *IEEE Systems Journal*, vol. 14, no. 2, pp. 3001–3010, 2019.

He Huang received the B.Eng. from the School of Electrical Engineering, Xi'an Jiaotong University in 2019, and the MSc. degree in Electrical and Electronic Engineering from Nanyang Technological University in 2020. He is currently pursuing a Ph.D. degree with the School of Electrical and Electronic Engineering in Nanyang Technological University. His research interests include data analytics and machine learning with applications in indoor localization, smart sensing and Internet of Things.

Jianfei Yang received the B.Eng. from the School of Data and Computer Science, Sun Yat-sen University in 2016, and the Ph.D. degree from Nanyang Technological University (NTU), Singapore in 2021. He received the best Ph.D. thesis award from NTU. He used to work as a senior research engineer at BEARS, the University of California, Berkeley. His research interests include deep transfer learning with applications in Internet of Things and computer vision. He won many International AI challenges in computer vision and interdisciplinary research fields. Currently, he is a Presidential Postdoctoral Research Fellow and an independent PI at NTU.

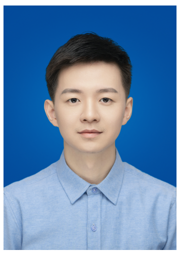

Xu Fang received the B.S. degree in Electrical Engineering from the Beijing Forestry University, China, in 2013, the M.Sc in Control Theory and Control Engineering from BeiHang University, China, in 2016, and the Ph.D. degree at the school of Electrical and Electronic Engineering, Nanyang Technological University, Singapore, in 2021. He is currently a Research Fellow with Nanyang Technological University, Singapore, under the Wallenberg-NTU Presidential Postdoctoral Fellowship. His research interests include cooperative control, unmanned systems, network localization, and robot navigation.

Hao Jiang received the B.S. and Ph.D. degrees from Xiamen University, Fujian, China, in 2008 and 2013, respectively. He is currently a professor with the College of Electrical Engineering and Automation, Fuzhou University. His research interests include artificial intelligence and machine learning with applications in indoor navigation, computer vision, fault diagnosis and mobile computing.

Lihua Xie received the B.E. and M.E. degrees in electrical engineering from Nanjing University of Science and Technology in 1983 and 1986, respectively, and the Ph.D. degree in electrical engineering from the University of Newcastle, Australia, in 1992. Since 1992, he has been with the School of Electrical and Electronic Engineering, Nanyang Technological University, Singapore, where he is currently a professor and served as the Head of Division of Control and Instrumentation from July 2011 to June 2014. He held teaching appointments in the Department of Automatic Control, Nanjing University of Science and Technology from 1986 to 1989 and Changjiang Visiting Professorship with South China University of Technology from 2006 to 2011.

Dr Xie's research interests include robust control and estimation, networked control systems, multi-agent control and unmanned systems. He has served as an editor of IET Book Series in Control and an Associate Editor of a number of journals including IEEE Transactions on Automatic Control, Automatica, IEEE Transactions on Control Systems Technology, and IEEE Transactions on Circuits and Systems-II. Dr Xie is a Fellow of IEEE and Fellow of IFAC.